

# 4D WARPING FOR ANALYSING MORPHOLOGICAL CHANGES IN SEED DEVELOPMENT OF BARLEY GRAINS

Rainer Pielot, Udo Seiffert

*Leibniz-Institut für Pflanzengenetik und Kulturpflanzenforschung (IPK)  
Corrensstraße 3, D-06466 Gatersleben, Germany*

Bertram Manz<sup>2</sup>, Diana Weier<sup>1</sup>, Frank Volke<sup>2</sup> and Winfriede Weschke<sup>1</sup>

<sup>1</sup> *Leibniz-Institut für Pflanzengenetik und Kulturpflanzenforschung (IPK)  
Corrensstraße 3, D-06466 Gatersleben, Germany*

<sup>2</sup> *Fraunhofer Institut für Biomedizinische Technik (IBMT)  
Ensheimer Str. 48, D-66386 St. Ingbert/Saar, Germany*

Keywords: Warping, NMR, registration.

Abstract: NMR imaging allows to obtain 3D-images by non-invasive treatment of biological structures. In this study intensity-based warping is evaluated by comparing it to landmark-based warping for a four-dimensional analysis of morphological changes in seed development of barley. The datasets of barley grains are obtained at certain development stages by NMR. Warping algorithms reconstruct intermediate physically non-measured stages. The landmark-based procedure consists of automatic definition of landmarks and subsequent distance-weighted warping. The intensity-based approach uses iterative intensity-based warping for definition of the displacement vector field and distance-weighted volume warping for generation of the virtual intermediate dataset. The approaches were tested with four datasets of barley at different development stages. As a result, the intensity-based approach is highly applicable for analysis of morphological changes in NMR datasets and serves as a tool for an extensive 4D analysis of seed development in barley grains.

## 1 INTRODUCTION

The accurate four-dimensional analysis of developing biological structures requires adequate techniques. In case of high-resolution NMR scans of biological structures, 4D warping can serve as a tool for visualization of morphological changes (Thompson and Toga, 1998; Shen and Davatzikos, 2003; Toga and Thompson, 2003; Shen, 2004). Analysis of seed development of barley encloses the detection of complex morphological change patterns. Therefore we investigate fast and robust warping strategies for applicability in biological image processing. Warping is a class of image processing techniques, which deals with nonlinear geometric transformations. According to the determination of the spatial correspondence between a source and a target image, warping algorithms can

be divided into two classes (Toga, 1998, Maintz and Viergever, 1998): Model-based approaches use high-level information, such as point landmarks (Bookstein, 1989; Franz et al., 1999; Whitbeck and Guo, 2006), contours (Subsol, 1998; Wang et al., 2004) and surfaces of anatomical structures (Davatzikos, 1996; Thompson and Toga, 1996, 2002). In contrast, intensity-based warping methods maximize local gray value correlation to match the source to the target image (Bajcsy and Kovacic, 1989; Ashburner et al, 1999). Hybrid approaches try to combine model-based and intensity-based techniques (Johnson and Christensen, 2002). The major drawback of pure intensity based methods is the incapacity to handle large deformations. To overcome these limitations, Christensen et al. have published (in 1996) a viscous fluid based warping procedure, which allows highly nonlinear, but

smooth and topology preserving, deformations with a relatively high computational cost. A faster derivative of the viscous fluid registration was published by Bro-Nielsen and Gramkow in 1996 using a convolution filter in a scale-space framework (Bro-Nielsen and Gramkow, 1996). Another well-known approach of iteratively registering an image is the “Demon’s Algorithm” (Thirion, 1996, 1998), which can be considered as an approximation of the viscous fluid registration (Bro-Nielsen and Gramkow, 1996).

The time- and memory consuming step of fluid registration procedures is solving the linear PDE. In this study we present new iterative approach that performs the calculation of the displacement vector field (DVF) by bloc-matching and by minimizing a threshold function to get fast computation and few memory consumption. Distance-weighted warping performs the subsequent volume transformation of all voxels of the source image to the target image using the DVF as geometric information. The method was applied to gradient images, which are obtained from the gray value datasets (see Material & Methods).

This approach was compared to a fast and robust landmark-based approach with an iterative intensity-based approach. The manual definition of a sufficient amount of landmarks is subjective and time-consuming, therefore the 3D landmarks were automatically generated. The automatic definition of an adjustable number of landmarks is based on 3D differential operators (Rohr, 1997).

NMR-imaging allows to obtain 3D-images by non-invasive treatment of the biological material, and was successfully applied to barley grains (Glidewell, 2006). The aim of the presented study is the evaluation of two different warping strategies for transformation of interindividual NMR datasets of barley grains at different development stages. The transformation helps to analyze morphological changes during seed development by reconstructing a complete time series of NMR datasets. The measured NMR datasets at distinct time points are serving as reference for the iterative warping procedure. The approaches were evaluated by calculation of global cross correlation and volume overlap index between the warped and the target dataset over time.

## 2 MATERIAL & METHODS

In this study 4 NMR datasets at different development stages are used (3 Days After Flowering (DAF), 3.5, 9, and 10 DAF). The datasets are divided into two groups to examine seed development at an early stage (3 DAF + 3.5 DAF) and at a relatively late stage (9 DAF + 10 DAF). Each group is processed separately and independently, i.e. 3 DAF is transformed to 3.5 DAF and 9 DAF is warped to 10 DAF.

Both pairs of datasets are differing in size and represent different growth patterns, so that they were chosen out of 16 measured datasets as examples to demonstrate the method under dissimilar conditions. The reconstruction of seed development between 3 DAF and 3,5 DAF was chosen due to enormous morphological changes between these time points.

The general work flow is as follows: After obtaining the datasets, a manual rigid alignment of the 3D images to each other ensures best starting conditions. Then, as the first step in an iterative process, the gray value datasets were duplicated and the copies were converted to a gradient dataset. Subsequently the registration process generates the displacement vector field (DVF) to determine the spatial correspondence between the source and the target image. The last step is the volume warping of the non-converted source gray value dataset. The iteration cycle starts again with the gradient calculation of a copy of the warped dataset. After a predefined number of iterations the whole process stops. Fig. 1 shows the general scheme.

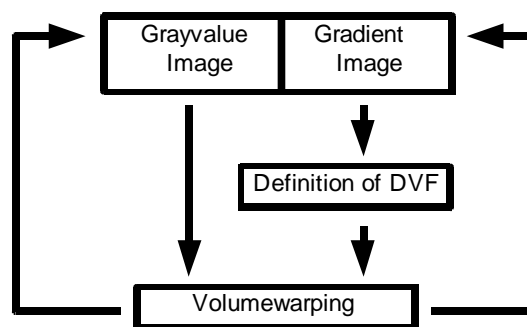


Figure 1: Diagram of general work flow.

### 2.1 NMR-Imaging and Image Preprocessing

A Bruker DMX 400 NMR spectrometer (Bruker, Rheinstetten, Germany) with a Micro2.5 imaging

probe was used for the MRI (Magnetic Resonance Imaging) experiments. All three-dimensional images were recorded using a standard T1-weighted 3D spin-echo pulse sequence with a repetition time  $T_r$  of 300 ms and an echo time  $T_e$  of 4.4 ms. The image resolution was 31  $\mu\text{m}$  along the axial and 16  $\mu\text{m}$  along the transverse directions and dimensions of the datasets are 512x175x256 voxels (9 DAF, 10 DAF) and 194x124x256 voxels (3 DAF, 3.5 DAF), depending on the size of the biological structures.

The datasets were converted to a gray value resolution of 8 bit, contrast enhanced and manually put into the same orientation. Afterwards they were manually aligned to each other, as an important prerequisite for the registration process.

## 2.2 Landmark-based Approach

The automatic definition of landmarks is based on 3D operators for the detection of point landmarks in MR images. The operator consists of first partial derivatives of the voxels and detects corners and saddle-points of biological structures. To ensure correct correspondence of the detected reference points, a 3D grid is placed on each dataset to define non-overlapping subvolumes. Only if a corresponding subvolume contains a reference point in both datasets, these reference points are defined as landmarks. The spatial difference of a pair of corresponding landmarks denotes a displacement vector. For the time-series the length of the displacement vectors are successively reduced to realize a reverse „growth“. At each timepoint, a volume warping is performed.

The displacement vectors describe the DVF, therefore the same distance-weighted volume warping method is used as in the intensity-based approach.

## 2.3 Iterative Intensity-based Approach

As the first step in an iterative process, the gray value datasets were duplicated and the copies were converted to a gradient dataset. Subsequently the registration process generates the displacement vector field (DVF) to determine the spatial correspondence between the source and the target image. The last step is the volume warping of the non-converted source gray value dataset. The iteration cycle starts again with the gradient calculation of a copy of the warped dataset. After a

predefined number of iterations the whole process stops.

Pretests without conversion into gradient images showed poor results probably due to differing contrast in the NMR datasets.

The first step of the iteration cycle is to calculate the gradient image of the source and the target dataset by application of a sobel mask. Therefore the registration is performed on the gradient dataset and not on the original gray value datasets. Based on linear elasticity properties of a deformed body, which are described by the Navier-Stokes equation, the gradient of local similarity between the target and the deformed image represents the body forces. The strength of deformation is regulated by the internal forces. To overcome the limitations of only small deformations, the whole process becomes iterative by adding time to it.

The presented approach changes this model to a simpler and faster algorithm by reducing the core problem of time-consuming solving of PDEs to a minimization problem. The internal forces are simplified to a simple threshold function  $s(\mathbf{u}(\mathbf{x}, t))$ :

$$s(\mathbf{u}(\mathbf{x}, t)) + \mathbf{b}(\mathbf{u}(\mathbf{x}, t)) = \min \quad (1)$$

The body forces  $\mathbf{b}(\mathbf{u}(\mathbf{x}, t))$  are determined by the local sum of squared differences of the voxel values of the source dataset  $S$  and the target dataset  $T$ :

$$\mathbf{b}(\mathbf{u}(\mathbf{x}, t)) = \sum (S(\mathbf{x} + \mathbf{u}(\mathbf{x}, t)) - T(\mathbf{x}))^2 \quad (2)$$

and the threshold function is defined as:

$$s(\mathbf{u}(\mathbf{x}, t)) = \begin{cases} \infty & (\sum |\mathbf{u}(\mathbf{x}, t)|) > c \\ 0 & (\sum |\mathbf{u}(\mathbf{x}, t)|) < c \end{cases} \quad (3)$$

where  $c$  depicts a predefined threshold value. In this study the non-critical value of  $c$  was set to 5, therefore the maximal length of a displacement vector cannot exceed this value. In contrast to common iterative elastic matching algorithms, the displacement vectors are only determined for rigid displacement of local subvolumes of 10 x 10 x 3 voxel. Therefore the calculation of the DVF can be described as a very fast bloc-matching process.

For each local subvolume the best displacement is determined by minimizing eq. (1). After the registration procedure the DVF contains  $M$  vectors, each vector can be taken as the spatial difference between the points  $v_i$  in the target image and  $x_i$  in the source image. These points are called registration points.

The volume warping requires a robust and fast warping method to handle a large number of displacement vectors obtained by the registration step. We chose a distance-weighted warping algorithm to ensure mathematical robustness even with a high number of displacement vectors. The smoothness of the transformation is controlled by a global parameter.

The transformation function  $r(\mathbf{x})$  of the used warping method calculates the displacement of each voxel  $\mathbf{x}$  by the weighted sum of all displacement vectors:

$$r(\mathbf{x}) = \mathbf{x} + \frac{\sum_{i=0}^{M-1} w_i(\mathbf{x})[\mathbf{v}_i - \mathbf{x}_i]}{\sum_{i=0}^{M-1} w_i(\mathbf{x})} \quad (4)$$

The weighting function consists of a global weighting factor  $\beta$  and the Euclidean distance of the point  $\mathbf{x}$  to the reference point  $\mathbf{x}_i$ :

$$w_i = e^{\beta \sqrt{[(x-x_i)(y-y_i)(z-z_i)]}} \quad (5)$$

To decrease computational efforts, only reference points with a distance value smaller than a given threshold are used for further calculation. The global weighting factor  $\beta$  shapes the transformation: a high value results in local and coarse transformations whereas a low value yields smooth displacements. For the intensity-based approach we set  $\beta$  to 0.02. In case of the landmark-based approach a value of 0.10 is used.

After generation of the gray value dataset by this distance-weighted warping algorithm, the warped dataset is duplicated, then the copy is converted into a gradient dataset and fed into the next iteration cycle. Due to the lack of a reliable convergence criterion, the whole process was stopped after a predefined number of 30 iteration cycles.

### 3 RESULTS

All calculations were performed on an SMP Opteron 850 system with Linux 2.6.13. In case of the early development stage the intensity-based approach uses 17,136 vectors (landmark-based: 1,071 landmarks) and in case of the late development stage 57,600 vectors (landmark-based: 3,120 landmarks) are used for the volume warping.

In case of the early development stage fig. 2 shows one single slice ( $z=126$ ) out of the volumes. The original NMR datasets were cropped at their left ends, because the caryopsis does not reach the glumes completely. The upper row shows on the left the target and on the right the source dataset with an automatically generated outer contour of the target. The lower row shows the warped dataset at the same  $z$ -position after 5 resp. 30 iteration cycles. It can be seen, that the warping process simulates nonlinear growth of the caryopse, until the most left part of the caryopse reaches the position of the same structure in the target dataset.

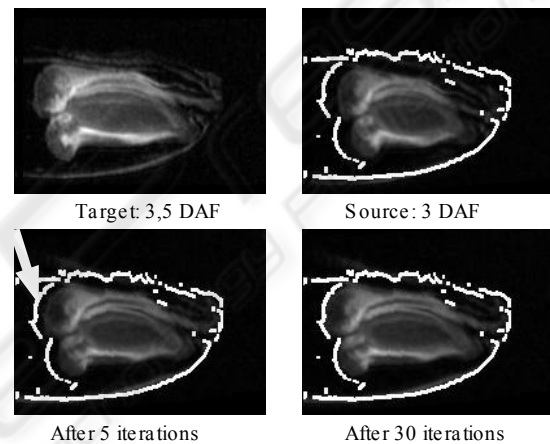


Figure 2: Single slice ( $z=126$ ) from NMR datasets (early development stage). Upper row: Target dataset and source dataset with outer contour of target. Lower row: Warped dataset after 5 and 30 iterations. The arrow depicts the outer contour of the caryopse to demonstrate the iterative process of transformation.

Fig. 3 shows for the late development stage the results of the intensity-based approach one single slice ( $z=126$ ) of the target dataset (upper row, left) and on the right the corresponding slice of the source dataset together with the outer contour of the target dataset. In the middle row the warped datasets after 5 and 30 iterations resp. are depicted. For a better evaluation the lower row shows magnifications. It can be seen, that the shapes of the biological structures became more similar to each other.

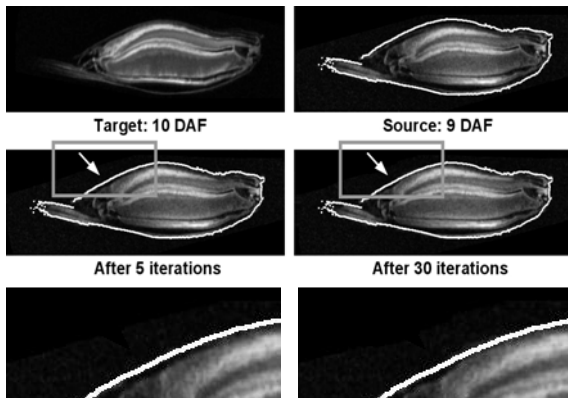


Figure 3: Single slice ( $z=126$ ) from NMR datasets (late development stage). Upper row: Target dataset and source dataset with outer contour of target. Middle row: Warped dataset after 5 and 30 iterations. The arrows depict a prominent location to see the iterative process of transformation. Lower row: Magnifications of the marked regions.

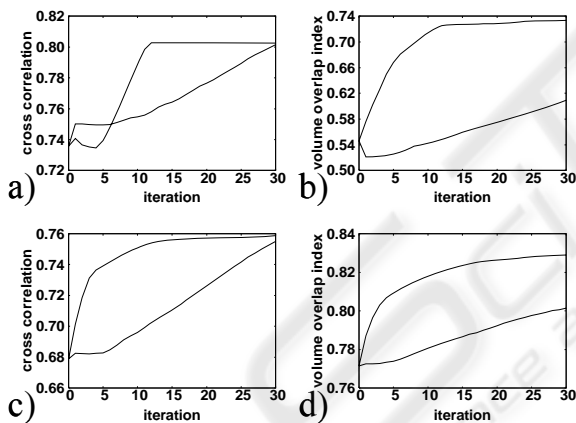


Figure 4: Increase of the global cross correlation coefficient and the volume overlap index during the iterations. The thicker curve depicts the results of the intensity-based approach and the thinner curve the results of the landmark-based approach. The iterations were stopped after 30 cycles. a) and b): early development stage, c) and d): late development stage.

The increase of the global cross correlation coefficient (cc) and the volume overlap index (voi) is shown in Fig. 4. The global cross correlation measures the similarity of the global gray value distribution, whereas the volume overlap index quantifies the 3D geometric correspondence. In case of the intensity-based approach, a rapid increase of similarity in terms of the used quality functions shows a strong transformation at the beginning of

the iterations. After about 15 iterations the similarity increases only slightly. In case of landmark-based warping the increase is more or less linear after about 5 iterations. However, best results after 30 iterations are obtained by the intensity-based approach.

The increase of similarity in terms of the used similarity functions is summarized in tab. 1 (early development stage) and tab. 2 (late development stage).

Table 1: Increase of similarity (early development stage). The global cross correlation coefficient before warping between target and source dataset was 0.7359 and the volume overlap index was 0.5462.

	Intensity-based		Landmark-based	
	cc	voi	cc	voi
After 5 iterations	0.7394 +0.48%	0.6680 +22.30%	0.7495 +1.85%	0.5256 -3.77%
After 30 iterations	0.8025 +9.05%	0.7335 +34.29%	0.8014 +8.90%	0.6091 +11.52%

Table 2: Increase of similarity (late development stage). The global cross correlation coefficient before warping between target and source dataset was 0.6790 and the volume overlap index was 0.7716.

	Intensity-based		Landmark-based	
	cc	voi	cc	voi
After 5 iterations	0.7419 +9.26%	0.8115 +5.17%	0.6826 +0.53%	0.7740 +0.31%
After 30 iterations	0.7691 +13.27%	0.8375 +8.54%	0.7551 +11.21%	0.8014 +3.86%

## 4 CONCLUSIONS

The aim of this study was the investigation of 4D warping of interindividual NMR datasets of barley grains at different development stages. The transformations help to visualize morphological changes during seed development of barley. We have developed and evaluated an iterative procedure to generate virtual datasets using measured NMR datasets as reference. Similarity measurements by applying global cross correlation and volume overlap index as quality functions show an increase during the iterations. In case of our new method, the increase of similarity is not linear in terms of the

used similarity functions. This is a property of the used intensity-based warping method. However, up to now, it is more likely that the growth of the structures in barley grains between the presented timepoints is nonlinear. The landmark-based approach shows a linear increase in terms of the quality functions, but produces suboptimal results after a given number of iterations.

The presented algorithm will serve as a tool for further four-dimensional analysis of seed development in barley: For further 4D analysis expression data will be incorporated into the virtual NMR datasets to visualize time-dependent localization of e.g. metabolites during development. For this task the presented iterative procedure appears to be highly suitable for time-dependent transformation of one development stage to another and may prove to be a useful tool to make morphological changes during seed development accessible for further analysis.

## ACKNOWLEDGEMENTS

This work was supported by a grant of the Deutsche Forschungsgemeinschaft (DFG) (FKZ WE 1608/2-1). We would like to thank Dr. Bernd Brückner (IfN Magdeburg) for help with the calculations.

## REFERENCES

- Ashburner, J., Andersson, J.L.R., Friston, K.J., 1999. High-dimensional image registration using symmetric priors, *NeuroImage*, 9:619-628
- Bajcsy, R., Kovacic, S., 1989. Multiresolution elastic matching, *Computer Vision, Graphics and Image Processing* 46:1-21
- Bookstein, F.L., 1989. Principal warps: Thin-plate splines and the decomposition of deformations, *IEEE Transactions on pattern analysis and machine intelligence* 11:567-585
- Bro-Nielsen, M., Gramkow, C., 1996. Fast fluid registration of medical images, In *Visualization in Biomedical Computing*, 1131:267-276
- Christensen, G.E., Rabbitt, R.D., Miller, M.I., 1996. Deformable templates using large deformation kinematics, *IEEE Transactions on Image Processing* 5(10):1435-1447
- Davatzikos, C., 1996. Spatial normalization of three-dimensional brain images using deformable images, *J. Comput. Assist. Tomogr.*, 20(4):656-665
- Franz, S., Rohr, K., Stiehl, H.S., Kim, S.-I., Weese, J., 1999. Validating point-based MR/CT registration based on semi automatic landmark extraction. In *CARS'99*, pp. 233-237
- Glidewell, S.M., 2006. NMR imaging of developing barley grains, *Journal of Cereal Science*, 43:70-78
- Johnson, H.J., Christensen, G.E., 2002. Consistent landmark and intensity-based image registration, *IEEE Transactions on medical imaging*, 21(5):450-461
- Maintz, J.B.A., Viergever, M.A., 1998. A Survey of Medical Image Registration, *Med. Image Anal.*, 2(1):1-37
- Rohr, K., 1997. On 3D differential operators for detecting point landmarks, *Image and Vision Computing*, 15(3): 219-233
- Shen, D., 2004. 4D Image warping for measurement of longitudinal brain changes. In *Proceedings of the 2004 IEEE International Symposium on Medical Imaging*, pp. 904-907
- Shen, D., Davatzikos, C., 2003. Measuring temporal morphological changes robustly in brain MR images via 4-dimensional template warping, *NeuroImage*, 21:1508-1517
- Subsol, G., 1998. Crest lines for curve-based warping. In *Brain warping*, Academic Press, San Diego
- Thirion, J.-P., 1996. Non-rigid matching using demons, *Proc. Int. Conf. Computer Vision and Pattern Recognition (CVPR'96)*
- Thirion, J.-P., 1998. Image matching as a diffusion process: an analogy with maxwell's demons, *Medical Image Analysis*, 2:243-260
- Thompson, P.M., Toga, A.W., 1996. A surface-based technique for warping three-dimensional of the brain, *IEEE Transactions on Medical Imaging*, 15(4):1-16
- Thompson, P.M., Toga, A.W., 1998. Anatomically-driven strategies for high-dimensional brain image warping and pathology detection, In *Brain Warping* (Toga, A.W., Ed.), pp. 311-336, Academic Press, San Diego
- Thompson, P.M., Toga, A.W., 2002. A framework for computational anatomy, *Computing and Visualization in Science*, 5:13-34
- Toga, A.W., 1998. *Brain warping*, Academic Press, San Diego
- Toga, A.W., Thompson, P.M., 2003. Temporal dynamics of brain anatomy, *Annual Review of Biomedical Engineering*, 5, 119-145
- Wang, A.Y., Leow, A.D., Protas, H.D., Toga, A.W., Thompson, P.M., 2004. Brain warping via landmark points and curves with a level set representation, In *Proc. Medical Imaging Computing and Computer Assisted Intervention (MICCAI)*, 2004
- Whitbeck, M., Guo, H., 2006. Multiple landmark warping using thin-plate splines. In *IPCV'06*, pp. 256-263